JOURNAL OF APPLIED ELECTROCHEMISTRY 13 (1983) 669–678

The impedance of the lithium-thionyl chloride primary cell

M. HUGHES, S. A. G. R. KARUNATHILAKA, N. A. HAMPSON

Chemistry Department, University of Technology, Loughborough, Leics. LE11 3TU

T. J. SINCLAIR

Procurement Executive, Ministry of Defence, Royal Armament Research and Development Establishment, Fort Halstead, Sevenoaks, Kent.

Received 22 September 1982

The impedances of nominally fully charged and partially discharged $Li/SOCl_2$ cells have been measured in the frequency range 10 kHz–6 mHz. The data have been interpreted using an analogue technique in terms of the most probable cell reactions. The possibilities of state-of-charge tests based on the impedance technique are discussed. The most promising parameter for a residual capacity test in the region 100–90% is the double-layer capacitance.

Nomenclature

θ_1	charge-transfer resistance of the positive electrode (Ω)
θ_{Li}	charge-transfer resistance of the Li electrode (Ω)
R	gas constant ($J\,mol^{-1}K^{-1}$)
T	temperature (K)
z	number of electrons
F	Faraday
I_0	exchange current of the cell (Acm^{-2})
k^0	apparent standard state constant
C_{Li^+}	concentration of Li^+
α	charge-transfer coefficient
V	volume of electrolyte (dm^{-3})
W	weight of $SOCl_2$ in cell (g)
σ	Warburg diffusion ($\Omega\,s^{-1/2}$)
C_{dl_1}	double-layer capacitance of Li electrode (F)
R_Ω	ohmic resistance of cell (Ω)
C_{dl_2}	double-layer capacitance of $SOCl_2$ electrode (F)
θ_2	charge-transfer resistance of the $SOCl_2$ (Ω)
R_I	internal resistance in the analogue Fig. 8 (Ω)
C_x	external series capacitor in the analogue Fig. 8 (F)
x	number of coulombs passed

1. Introduction

Cells based on lithium anodes (negatives) have become important to contemporary primary cell technology because of their high potentials together with long shelf lives and with high specific energies. The literature of lithium based cells have been reviewed [1–3] and it is clear that certain depolarisers are becoming established as cathodes for particular specific applications. The problem of state-of-charge (and quality) monitoring is an important aspect of all electrochemical storage devices. We have been exploring the impedance technique as a suitable monitor for such fully sealed devices, [4] and recently we have reported the results of our work with Li/CuO [5] and Li/SO_2 [6].

The lithium primary cell containing depolarisers involving halogens have potentials in excess of 3 V and consequently are attractive for those applications which require ultra high specific energies. Depolarisers described include SO_2Cl_2/Cl_2 [7] and $SOCl_2/BrCl$ [8]. However, Klinedinst [9] has reported that the simple combination of $Li/SOCl_2$ is capable of yielding current densities well in excess of $500\,mAcm^{-2}$. Although the $Li/SOCl_2$ combination has a marginally reduced life over other halo-combinations [9], it was con-

0021-891X/83 $03.00 + .12.

sidered that this cell was of sufficient interest to merit an investigation of the impedance. This paper records our results.

2. Experimental procedure

The cell used was type LA30944 LAA-1, AA size (GTE Products Ltd.). The depolariser was absorbed onto acetylene black (~ 90%) bound with Teflon (~ 10%) which was supported on a nickel screen. The cell format was the bobbin type (in which the $C/SOCl_2$ forms a central cylindrical shape). Separation of the positive and negative electrodes was by non-woven glass fibre paper, (~ 0.1 mm thick) the cell element being contained in a stainless steel can. The electrolyte is $LiAlCl_4$ (~ 1.7 mol dm^{-3} in $SOCl_2$). The cell had a nominally rated capacity of 1.9 Ah and an operating voltage of 3.6 V within a range of currents between 20 and 50 mA.

The apparatus and procedures by which the impedance of the cell was measured poised at the equilibrium potential after various amounts of charge had been removed under galvanostatic conditions have been described [10]. In the present experiments, the cell was discharged at 25 mA until the necessary charge as measured on a coulometer had been removed. At least 24 h was allowed to elapse for diffusional processes within the cell to become completed before the commencement of the a.c. experiment.

3. Results

The impedance spectra observed at the various states-of-discharge differed throughout the whole range, nominally 0 to 120% discharged (at 25 mA).

Figure 1 shows the impedance spectrum of an undischarged cell. This cell had stabilized for 9 months since manufacture and represents a fully equilibrated response. It consists of a flattened semicircular shape (10 kHz to 10 Hz) terminating in a horizontal line (10 Hz to 1 Hz) followed by a low frequency region which is subject to considerable scatter. When a few per cent (1–2%) of the nominal cell capacity had been removed, the low frequency region becomes well-defined, as shown in Fig. 2. The horizontal portion is apparently terminated by a loop which crosses the original semicircular locus twice before becoming quite

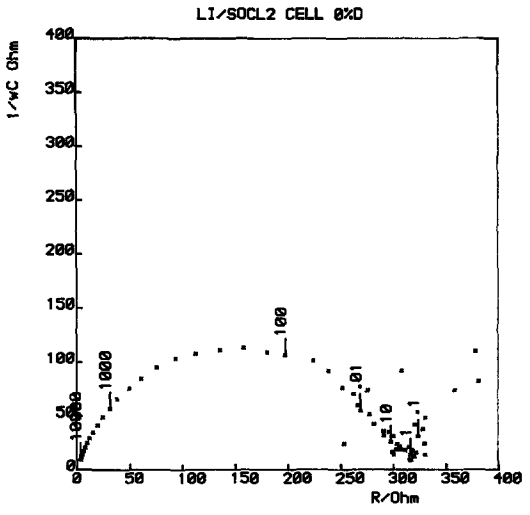

Fig. 1. Impedance loci of thionyl chloride cell (type LA 30944 LAA-1, AA size (GTE Products Ltd.)) undischarged at 23° C.

polarizable, the lowest frequency points at a few mHz rising almost vertically. Continued removal of charge results in the separation of the two semicircular shapes. Figure 3 shows a second semicircular shape that is recognisable which terminates in a polarizable region at very low frequency.

Although at 90% of the nominal capacity the second semicircle has become well-defined (and indeed Fig. 4 shows the absence of the horizontal region) it was preceded in the 90–95% range by extremely scattered results. We are unable to ascribe this scatter to experimental artefacts. The

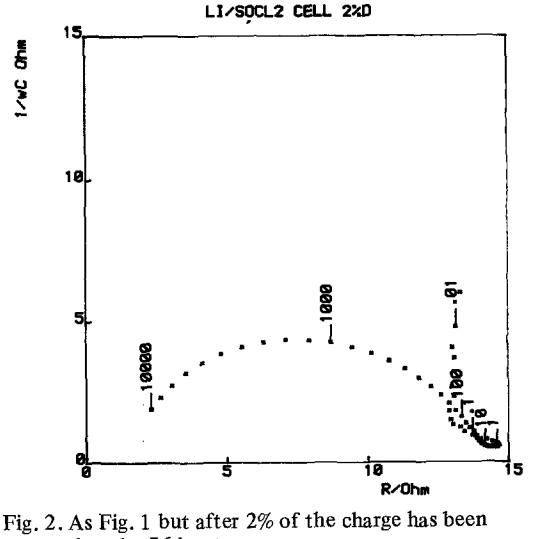

Fig. 2. As Fig. 1 but after 2% of the charge has been removed at the 76 h rate.

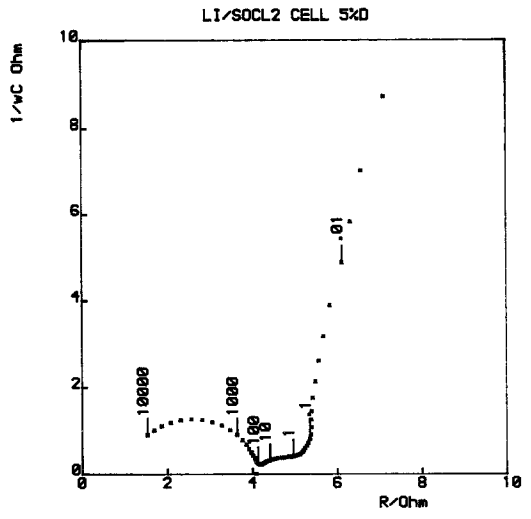

Fig. 3. As Fig. 1 but after 5% of the charge has been removed at the 76 h rate.

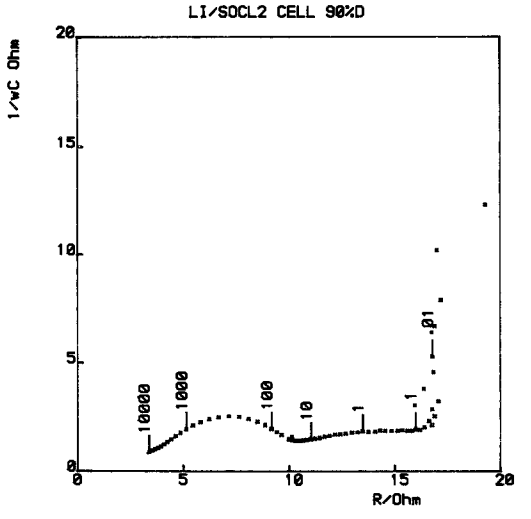

Fig. 5. As Fig. 1 but after 90% of the charge has been removed at the 76 h rate.

dual semicircular shape was maintained more or less throughout the region terminated by the withdrawal of the nominal capacity although Fig. 5 shows that at certain states-of-charges the second semicircle is very flat. At the nominal limit the second semicircular region has become very extensive and spans a resistance of 100 Ω over the frequency range 50 Hz–5 mHz (Fig. 6). A further feature at these lower states-of-charge is the very acute angle at which the locus comes from the real axis at the highest experimental frequency.

It was possible to obtain charge in excess of the nominal capacity from the cell. In fact the cell was discharged to a level of 120% of the rated capacity. Figure 7 shows the 110% discharged results. The interesting feature is the initial high frequency region at an angle of 45° with the real axis which subsequently increases and eventually shows the polarizable behaviour observed in all the experiments. At the 120% level this latter behaviour with considerable scatter was not really well defined. This was probably due to partial exhaustion of the active materials. This point was explored by opening the cell at the 120% level.

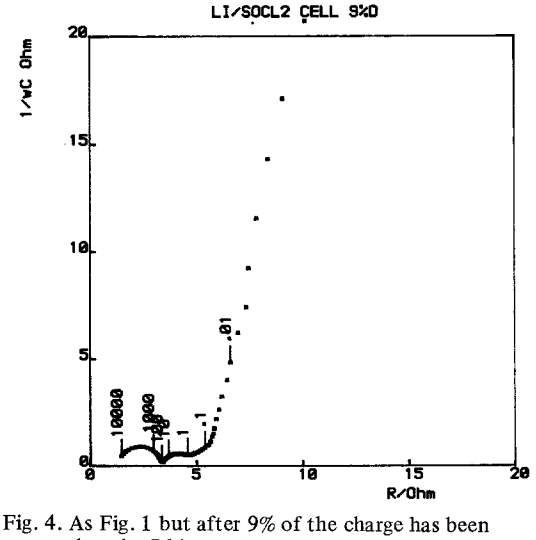

Fig. 4. As Fig. 1 but after 9% of the charge has been removed at the 76 h rate.

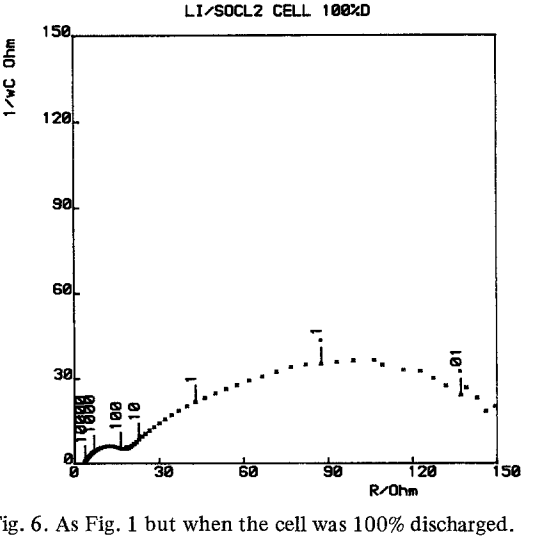

Fig. 6. As Fig. 1 but when the cell was 100% discharged.

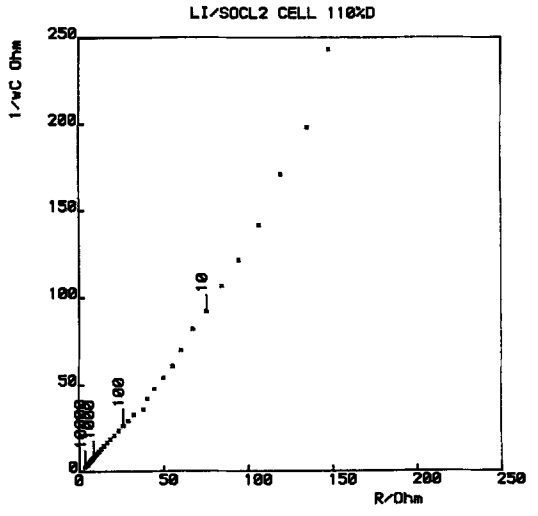

Fig. 7. As Fig. 1 but after charge 10% in excess of the nominal cell capacity had been removed at the 76 h rate.

We found residual thionyl chloride and lithium, however, it is likely that areas of the carbon were starved of reactant particularly adjacent to the positive current take-off connection.

4. Discussion

The experimental cell in this case is very complex and there are numerous papers which describe the products and reaction pathways of such a system. It is generally agreed [11, 12] that the main electrode reactions are

$$Li \longrightarrow Li^+ + e \qquad (1)$$

at the anode, and

$$2SOCl_2 + 4e \longrightarrow S + SO_2 + 4Cl^- \qquad (2)$$

at the cathode. In the case of reaction (1) the lithium (I) product may be ionic or solid LiCl, (at the electrode, an insoluble film of LiCl provides the barrier against parasitic anode corrosion).

Other reactions can be written for the cathode process but these are likely to be of minor importance. Sulphur dioxide product would be expected to react to give $S_2O_4^{2-}$ provided that the potential was sufficiently negative,

$$SO_2 + 2e \rightleftharpoons S_2O_4^{2-} \qquad (3)$$

In our experiments, it was only for states-of-charge when 10% or less of the nominal capacity remained in the cell, when (at 25 mA) the on-load voltage fell to a level corresponding to the equilibrium (3). Consequently, $S_2O_4^{2-}$ is only thermodynamically possible when the cell approaches the limit of the rated capacity.

The impedance loci reflect the electrochemistry associated with reactions (1) and (2). We have already shown that reaction (1) has the expected frequency response of a charge-transfer and subsequent diffusion in solution with the possible need for an additional capacitance term which arises from the presence of a partially blocking film at the electrode [5, 6]. This behaviour would produce a Randles circuit [13] in series with the electrochemical analogue representing the reaction (2).

Reaction (2) is itself a charge-transfer and diffusional process, but here the reactant is the solvent which is subject to ionization [14, 15]

$$SOCl_2 \rightleftharpoons SOCl^+ + Cl^- \qquad (4)$$

contributing to the electrolyte conductivity in addition to the added $LiAlCl_4$.

The cathodic reaction occurs on carbon in the adsorbed state and as such we would expect a reaction analogue in the sense of Laitinen and Randles [16]. This represents a reaction parallel to the solution reaction as occurring on the electrode surface between adsorbed species. A reaction capacitance and resistance appear in parallel to the solution phase process. The complete cell analogue is represented therefore by the circuit Fig. 8.*

The double-layer capacitance rises to a maximum at 40% state-of-charge and then diminishes. We suggest this is due to the surface becoming pitted as the reaction proceeds with attendant increase in area until products from the cell reaction are back precipitated at the electrode. The level at which this occurs corresponds with

* The approach adopted in this paper, the analogue technique, follows our earlier work with primary cells. It involves the estimation of a number of unknown circuit elements in the network which corresponds to the best representation of the electrochemistry. It is simpler operationally and fundamentally preferable to the technique of setting up a kinetic model for the cell reactions (porous electrodes and cell) and then finding the frequency response via the Laplace plane. With such complex technological systems to describe theoretically we have found the latter approach too daunting a problem. The analogue technique, although tedious, is manageable.

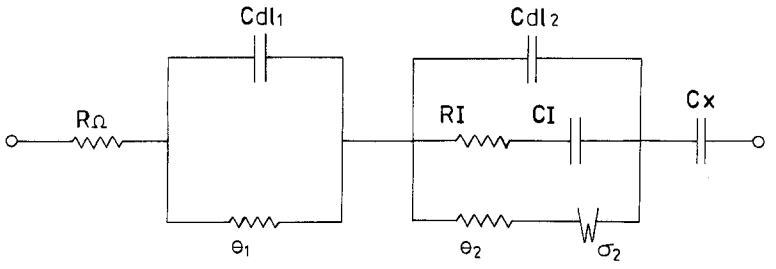

Fig. 8. Analogue circuit used in the computer modelling.

similar deposition processes at the $C/SOCl_2$ (*vide infra*).

The magnitudes of the circuit elements were evaluated using our computer techniques established for other primary cells which have been fully described [17]. The impedances of the cells at the various states-of-charge were matched over a minimum frequency range of 5 decades. The values of the computed circuit components are shown in Table 1.

Table 1 shows that the cell conforms to two models, that representing the high state-of-charge 100–98% and that representing the low state-of-charge down to 0%. Below 0% the model represented by Fig. 8 required modification. Results of the modelling are shown in Figs. 9–11.

4.1. *High states-of-charge*

The cell behaviour is dominated by the lithium electrode, the cathode limitations being undetectable. The effect of LiCl films was not detected within the experimental frequency range which was limited to 0.1 Hz due to pronounced scatter of results at low frequencies. Below 1 Hz, the cell behaviour was scattered. There was some indication of the presence of a loop in the capacitive region indicating the presence of an intermediate species. However, since it was only in the very high states-of-charge that these loci were observed, it can be concluded that the loop was due to either adsorption of electroactive species at the very negative or some unidentified intermediate species.

Table 1. Values of computed circuit components

State-of-charge (%)	θ_1 (Ω)	σ ($\Omega\,s^{-1/2}$)	C_{dl_1} (F)	R (Ω)	C_{dl_2} (F)	θ_2 (Ω)	R_I (Ω)	C_x (F)
100	260.1	114.1	3.3604E-6	15.43				
99	10.93	4.576	1.0058E-5	3.445				
98	10.63	6.695	8.2399E-6	2.3				
97	4.876	6.248	1.8148E-5	2.086				
96								
95	2.586	0.5529	2.5487E-5	1.508	2.4074E-2	0.6487	1E16	2.8
94								
93	2.104	0.6041	3.2046E-5	2.145	2.3915E-2	0.8440	1E16	3.0
92								
91	1.903	0.9503	3.9447E-5	1.447	2.3548E-2	0.8860	1E16	4.5
90	2.539	1.874	3.5829E-5	1.709	2.2784E-2	0.6982	1E16	1E12
80	2.219	1.484	6.6346E-5	2.128	1.4879E-2	0.6314	1E16	4.0
70	2.886	1.266	5.3283E-5	1.732	1.7647E-2	0.7697	1E16	4.1
60	1.629	1.103	7.5665E-5	1.681	1.9731E-2	0.6565	1E16	4.6
50	3.936	0.7745	1.0461E-4	1.927	2.1506E-2	1.594	1E16	1E12
40	2.026	1.82	1.889E-4	2.016	1.6570E-2	0.9029	3.4E16	4.0
30					3.06E-3	0.940		
20	2.419	3.544	2.3603E-4	1.884	8.631E-5	0.9812	4.254	3.0
10	3.988	17	6.3373E-5	3.787	4.9281E-4	2.873	10.74	3.2
0	15	23	6E-5	3.68	3.09E-3	41.62	1E16	1E16

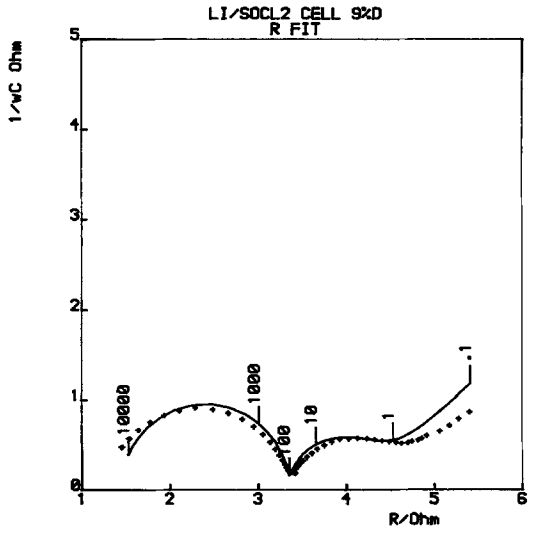

Fig. 9. Results of the computer fit for the $Li/SOCl_2$ cell when 95% charged.

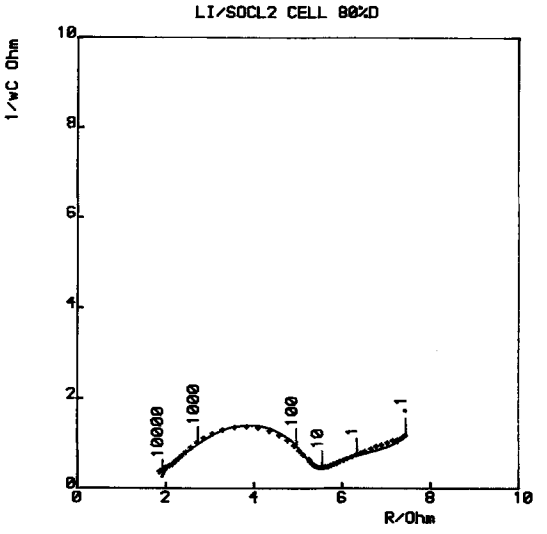

Fig. 11. Results of the computer fit for the $Li/SOCl_2$ cell when 10% charged.

Knowledge is lacking of the solution species in the $Li/SOCl_2$ system. The very rapid change in cell equilibrium potential ($\sim$ 100 mV) during the removal of the initial 2% of cell capacity and the abrupt change in the gradient of this curve thereafter (Fig. 12) however, indicates the presence of some unidentified electroactive component. Cell reactions which have been proposed do not seem to hold, as they do not generate a sufficiently high potential.

An alternative explanation is in terms of either cell additives or impurities. Commercially produced $Li/SOCl_2$ cells are certain to contain SO_2Cl_2, hence also Cl_2, the amounts of which vary with manufacturing practices.

The open circuit voltage (OCV) of the Li/Cl_2 in SO_2Cl_2 and the SO_2Cl_2 cells are 3.95 ± 0.02 V and 3.90 ± 0.02 V respectively. These voltages are similar to the original cell voltage under conditions of no load, and suggest that the cell contained some of these other more electroactive species.

The rapid fall of the OCV to that of one expected for a $Li/SOCl_2$ cell suggests that in the initial few per cent of discharge the more electroactive species are completely discharged leaving an $SOCl_2$ cathode material which would be expected to show the same potential as a $Li/SOCl_2$ system.

The breakdown of a film is unlikely to be the cause of the change in θ on discharging. There was no evidence for the presence of a significantly thick cathode film being developed on open circuit standing.

The experimental results show the impedance plots with R_Ω increasing with discharge and there was no evidence of potential increases on discharge. This is clear evidence that although a passivating layer which protects the Li must be present, the protective layer is undeveloped.

It can be concluded that some intermediate reactant is produced from the $SOCl_2$ which pref-

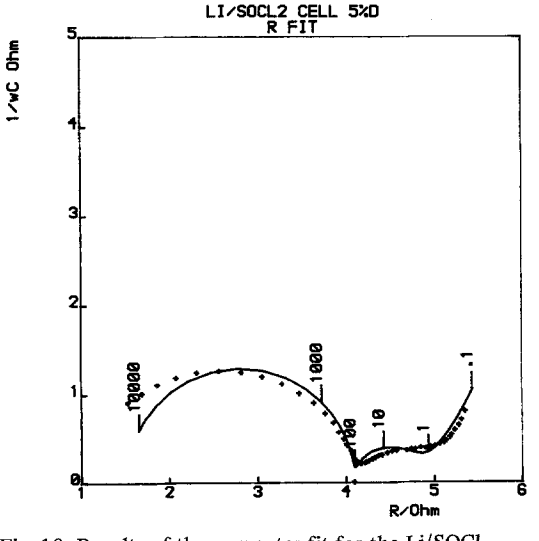

Fig. 10. Results of the computer fit for the $Li/SOCl_2$ cell when 91% charged.

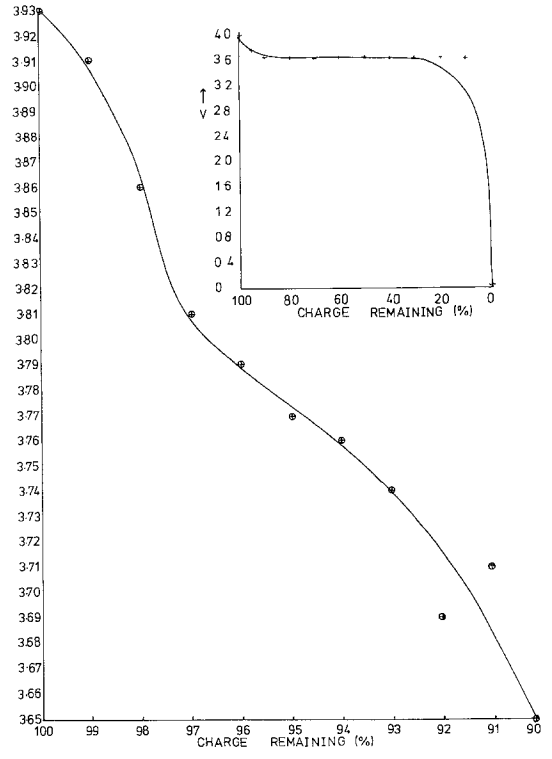

Fig. 12. Plot of cell OCV versus state-of-charge (under conditions of no load).

erentially reacts with the Li. Once this is removed there is no further evidence for enclosed loci in the impedance plots.

The magnitude of the charge-transfer resistance is initially high but rapidly falls as charge is withdrawn until at 97% charged it is only about 20% of the value before any charge has been withdrawn. The value of the Warburg coefficient changes very markedly in this region shrinking to about 6% of the initial value at 97% charged. This behaviour is entirely consistent with the initial presence of a layer of protective material across the electrode face. This material is probably LiCl. Before discharge the protective layer is well developed so that only about 5% of the electrode area is active for the anodic reaction as shown both by the decrease in charge-transfer resistance and the decrease in the Warburg coefficient.

4.2. *States-of-charge below 97%*

For states-of-charge below 97%, components of both electrode reactions were required in order to match the impedance loci. This can be ascribed to the fact that in our experiments the withdrawal of 3% of the nominal charge was necessary to remove sufficient of the anode film for the impedances of both electrodes to be of the same order of magnitude. We also found that the Warburg contribution corresponding to the Li electrode was small enough to be neglected. Presumably this is a consequence of the high active surface area of this electrode coupled with the very considerable lithium ion concentration of the electrolyte solution.

The interesting point which arises from the computer matches was that the adsorption capacitance was not required in the analogue. This is due to the fact that a very considerable amount of adsorption of reaction product occurred on the carbon as would be expected for the case of a strong sorption as occurs with carbon black.

A similar model fits the experimental facts until, charge 10% in excess of the nominal capacity had been withdrawn from the cell. In greater excess than 10% the model (Fig. 8) broke down completely and a satisfactory match could only be made using a single electrode system indicating the dominance of one of the electrodes (the failed one) in the cell analogue.

An interesting fact in the representation of the cell chemistry is that there was no need to take into account the electrode roughness until very considerable discharge had occurred. It is unlikely that the lithium electrode is smooth and the carbon is clearly porous. The apparent lack of porosity is curious; semicircles are somewhat flattened, however, it may be that in the higher states of charge the dual rôle of thionyl chloride as solvent and reactant results in a very major part of the reaction occurring at the front of the electrodes rather than inside. At low states-of-charge there is evidence of the high frequency semicircle coming off the real axis at less than 90°, showing some porosity. The better evidence of porosity, the Warburg behaviour at low frequency when pore penetration is more efficient is not available due to film formation. An examination of the lithium electrode at the termination of the discharge showed it to be porous.

It has not been found possible to fit the impedance to any kinetic scheme in order to obtain the characteristic constants for the electrode exchange reactions as was possible for the Li/SO_2 cell. The

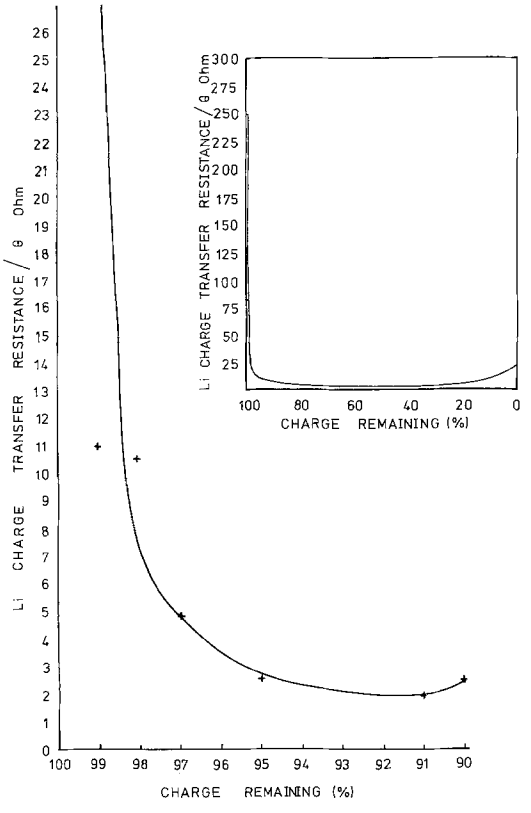

Fig. 13. Plot of the charge-transfer resistance of the Li electrode versus the charge remaining (%).

charge-transfer resistance for the Li electrode reaction fell rapidly in the region 100–90% state-of-charge and then became fairly constant before increasing markedly at 0% (Fig. 13). The double-layer capacitance on the Li showed a steady increase up to 50% state-of-charge and then decreased as shown in Fig. 14. The Warburg coefficient followed much the same changes as the charge-transfer resistance.

The double-layer on the $SOCl_2$ electrode is considerably in excess of that on the Li as would be expected. Indeed the difference of three orders of magnitude for the carbon black support cathode does not represent the true rates of the nominal electrode area. The double-layer on the cathode (Fig. 15) is constantly high until ~ 30–40% of the charge remains when it shrinks by ~ 2 orders of magnitude over a 10% removal of charge. This can be interpreted as the deposition of solid cell reaction products at the carbon considerably reducing the high area structure. The transition to the effectively planar electrode is accompanied by a

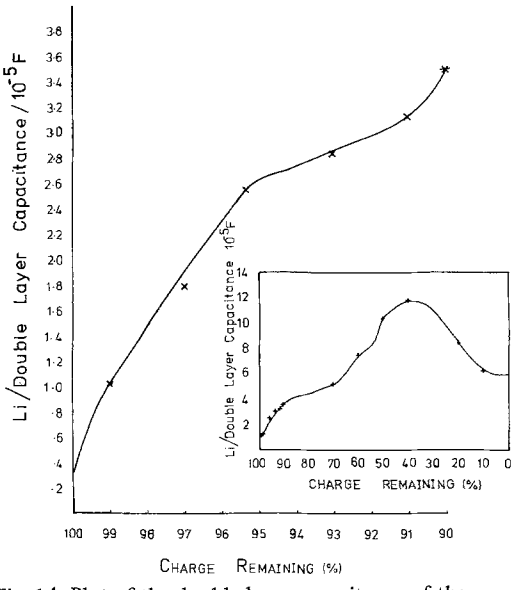

Fig. 14. Plot of the double-layer capacitance of the lithium electrode versus the charge remaining (%).

complementary fifty-fold increase in charge-transfer resistance. The discrepancy between the relative changes in charge-transfer resistance and double-layer capacitance is evidence for the majority of the reaction occurring at the front of the porous electrode, in short, it tends to react at a plane, i.e., a planar electrode.

4.3. *Double-layer capacitance of lithium*

Figure 14 shows that the double-layer capacitance on the Li increases to a maximum at 50% of the

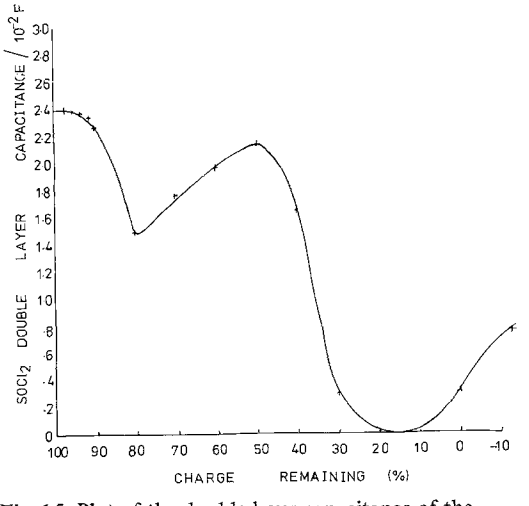

Fig. 15. Plot of the double-layer capacitance of the $SOCl_2$ versus the charge remaining (%).

fully-charged state and then falls. This is consistent with the $LiCl_{(s)}$ covering of the lithium electrode being stripped away at the very high states-of-charge to produce a more active surface of considerably greater area at which the electrochemistry can occur unhampered by a film. The marked electrode area increase is also consistent with a surface area enhancement due to the uneveness of the attack. The reduction in double-layer capacitance indicates that the electrode is being obscured probably by LiCl or alternatively some other of the electrode products e.g., S.

4.4. *Charge-transfer resistance of lithium*

The lithium charge transfer resistance initially falls very rapidly as charge is removed from the cell.

This is complementary to the change in double-layer capacitance and corresponds to the exposure of increasing surface of the electrode to the electrochemical process e.g., reaction (1). If the lithium ion remained in solution the charge-transfer resistance would decrease according to

$$\theta_{Li} = \frac{RT}{ZF} x \frac{1}{I_0} = \frac{RT}{Z^2F^2Ak^0C_{Li^+}^{1-\alpha}} \qquad (5)$$

Remembering that C_{Li^+} increases to the solubility limit of LiCl in $SOCl_2$ – as a consequence of the removal of the Li and the $SOCl_2$ as cell products – the change in θ_{Li} with state-of-charge. This argument leads to an expression for C_{Li^+} after x coulombs have been withdrawn from the cell

$$C_{Li^+} = (1.5 + x/FV)(1 - 60x/2FW) \qquad (6)$$

where V is the volume (in dm^{-3}) of the electrolyte in the cell and W is the weight of $SOCl_2$ in the cell. Putting Equation 6 in Equation 5 gives the change in θ with x due to concentration changes in solution. This function is shown in Fig. 16 assuming a value of 0.5 for the charge-transfer coefficient of the lithium electrode in thionyl chloride. The gradient of this curve obtained by differentation indicates a complex relationship involving an inverse cubic equation which has limited application in the present context. Comparing Figs. 13 and 16 for the actual state-of-charge vs. θ_{Li} relationship, and the theoretical one assuming planar Li and a simple charge-transfer mechanism indicates that this latter model is too simple. The

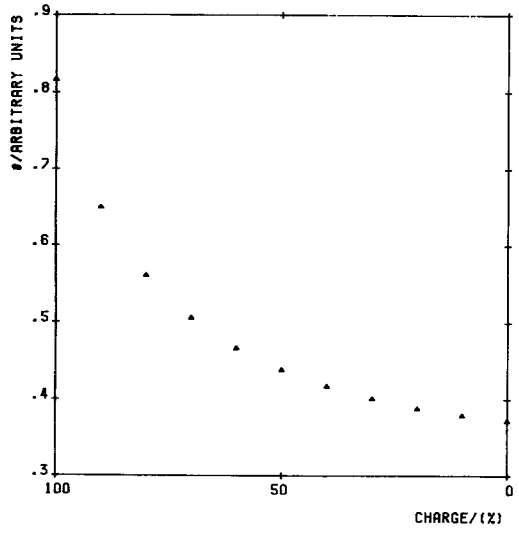

Fig. 16. The function, Equations 5 and 6 showing θ in arbitrary units against a notional state-of-charge.

geometry of the Li electrode is unlikely to remain planar and indeed our examination of the morphology of that electrode after some charge had been withdrawn from the cell is shown in Fig. 17. The SEM shows a very complex surface with porosity arising from intergrannular attack of the surface. Under these conditions it is unlikely that Equation 5 is obeyed in this simple form. The measured reduction in θ, is less than the calculated value in the initial stages of discharging in agreement with a developing surface area (porosity).

4.5. *The $SOCl_2$/C electrode*

The effects of the withdrawal of charge on the

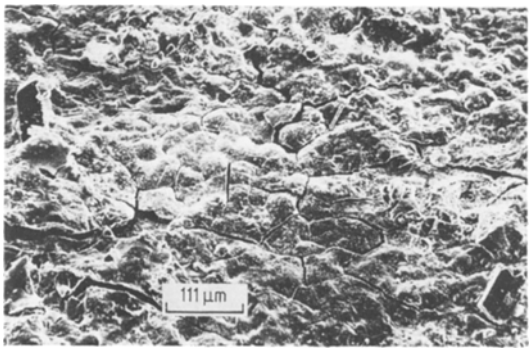

Fig. 17. SEM photograph of the Li electrode taken from a fully discharged lithium/thionyl chloride cell.

circuit elements of the C electrode are most interesting. Initially the double-layer capacitance is low, however, after a few per cent of the capacity has been removed it increases to the magnitude expected for a high area electrode. We can only conclude that initially only a small fraction of the carbon is really active, however, as the reaction proceeds the whole porous mass becomes involved. This suggests that the swelling of the carbon black with discharging which has been well-established [18], facilitates the reaction promoting the support of the cathodic reaction by the whole area. In the latter stages of discharge the double-layer capacitance once again shrinks. No reason is apparent except the utilization of the cathodic depolarizer.

4.6. *State-of-charge test*

Four parameters appear to be suitable bases for a state-of-charge test. Both the double-layer capacitance or the charge-transfer resistance on either electrode exhibits suitable changes in magnitude as current is withdrawn from the cell. The most conveniently measurable one is the charge-transfer resistance of the lithium electrode. Figure 13 shows that in the region to ~ 90% state-of-charge, a test should be relatively easy to formulate although the relationship between θ_1 and state-of-charge is not linear.

Conclusions

1. The Li–$SOCl_2$ cell can be represented as two electrode reactions.

2. The Li electrode is well-behaved over the whole range once the protective film (of LiCl) has been removed by discharging.

3. The C/$SOCl_2$ electrode is well-behaved to a 40% state-of-charge when the cell products (LiCl, $LiAlCl_4$) are apparently deposited in such a way as to coat the carbon rendering it planar.

4. The cell reactions are too complicated for the electrode kinetics *per se* to be evaluated.

5. A state-of-charge test for the cells can be formulated using either charge-transfer resistance or double-layer capacitance.

Acknowledgement

We are grateful to a referee for suggesting an alternative mechanism for one of the component cell reactions. This work has been carried out with the support of Procurement Executive, Ministry of Defence.

References

[1] B. Scrosati, *Electrochim. Acta* **26** (1981) 1559.
[2] N. Marincic, *Prog. Batteries Sol. Cells* **2** (1979) 40.
[3] R. J. Brodd and A. Kozawa, *Tech. Electrochem.* (1978) 200.
[4] S. A. G. R. Karunathilaka, N. A. Hampson, R. Leek and T. J. Sinclair, *J. Appl. Electrochem.* **10** (1980) 799.
[5] R. Leek, S. A. G. R. Karunathilaka, N. A. Hampson and T. J. Sinclair, Proceedings of Anglo-Czech Symposium on Fundamental Aspects and Analytical Applications of Electrochemical Detectors, Plenum Press, London (1982).
[6] M. Hughes, S. A. G. R. Karunathilaka, N. A. Hampson and T. J. Sinclair, *J. Appl. Electrochem.* **12** (1982) 537.
[7] R. M. Murphy, P. W. Krehl and C. C. Liang, 'Proceedings 16th Intersociety Energy Conversion Engineering Conference' Vol. 1. American Society Mechanical Engineers, New York (1981) p. 97.
[8] C. C. Liang, P. W. Krehl and D. A. Dauner, *J. Appl. Electrochem.* **11** (1981) 563.
[9] K. A. Klinedinst, *J. Electrochem. Soc.* **128** (1981) 2507.
[10] S. A. G. R. Karunathilaka, N. A. Hampson, R. Leek and T. J. Sinclair, *J. Appl. Electrochem.* **10** (1980) 357.
[11] J. C. Bailey and J. P. Kohut, 'Power Sources 8', (edited by J. Thompson) Academic Press, London (1981) p. 17.
[12] J. J. Auborn, K. W. French, S. J. Leiberman, V. K. Shah and A. Heller, *J. Electrochem. Soc.* **120** (1973) 1613.
[13] J. E. B. Randles, *Disc. Farad. Soc.* **1** (1947) 11.
[14] A. N. Dey and C. R. Schlaikjer, 26th Power Symposium, Atlantic City, 1974.
[15] A. N. Dey, *Electrochim. Acta* **21** (1976) 377.
[16] H. A. Laitinen and J. E. B. Randles, *Trans. Farad. Soc.* **51** (1955) 54.
[17] S. Kelly, N. A. Hampson, S. A. G. R. Karunathilaka and R. Leek, *Surf. Tech.* **13** (1981) 349.
[18] V. Manev, A. Nassalevska and R. Moshtev, *J. of Power Sources* **6** (1981) 337.